Materials Science & Engineering A 662 (2016) 492–505

Contents lists available at ScienceDirect

Materials Science & Engineering A

journal homepage: www.elsevier.com/locate/msea

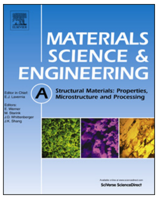

Effect of Li addition on the plastic deformation behaviour of AZ31 magnesium alloy

Govind Bajargan [a,b], Gaurav Singh [b], U. Ramamurty [b,c,*]

[a] Foundry Technology Division, Vikram Sarabhai Space Centre, Trivandrum 695022, India
[b] Department of Materials, Indian Institute of Science, Bangalore 560012, India
[c] Center of Excellence for Advanced Materials Research, King Abdulaziz University, Jeddah 21589, Saudi Arabia

ARTICLE INFO

Article history:
Received 11 February 2016
Received in revised form
17 March 2016
Accepted 18 March 2016
Available online 19 March 2016

Keywords:
Mg alloys
Li addition
Twinning
Dynamic recrystallization
Dynamic recovery
Slip system
Work hardening

ABSTRACT

The enhancement in the workability, if any, of a dilute Mg alloy, AZ31, with the Li addition is investigated by examining the hot deformation behaviour of AZ31 alloyed with 1, 3 and 5 wt% Li. Compression tests were conducted in the temperature, T, range of 150–400 °C and strain rates, $\dot{\varepsilon}$, ranging from 10^{-3} to $10^{+2}\ s^{-1}$. Experimental results show that the deformation behaviour can be divided into three T regimes. In the low T regime (150–200 °C), an increase in the Li content in AZ31 decreases the twin density with a concomitant enhancement in the non-basal or cross-slip activity. While high Li alloys exhibit low flow stress at low $\dot{\varepsilon}$ in this regime, an increase in $\dot{\varepsilon}$ increases strain hardening rate and twinning activity. Flow localization and shear band formation were observed in most of the alloys in this regime. Deformation in the intermediate T regime (250–300 °C) leads to dynamic recovery (DRY) at low $\dot{\varepsilon}$ and dynamic recrystallization (DRX) at high $\dot{\varepsilon}$, which are the softening mechanisms in Li containing alloys. In high T regime (350–400 °C), these alloys exhibit softening mechanisms similar to intermediate T regime but high Li alloys surprisingly exhibit higher flow stresses, which is attributed to the higher amount of Li in the solid solution, a result of the dissolution of Li containing precipitates. Non-basal slip and twinning at high $\dot{\varepsilon}$ occur uniformly with homogeneous DRX. A low activation energy for deformation of high Li alloys indicates that the Friedel-Escaig (F-E) mechanism as the rate controlling deformation mechanism. The onset of twinning was examined by the appearance of first local maxima before peak strain in $(d^2\sigma/d\varepsilon^2)$ vs. ε curves. Mechanisms responsible for the dependence of critical stress for the onset of DRX on T and $\dot{\varepsilon}$ are also discussed.

1. Introduction

Mg and its alloys have attracted considerable research attention in the recent past. A number of potential applications in aerospace and automobile industries, which accord a premium on high structural efficiency, are envisioned [1,2] for these alloys due to their lightweight. However, poor workability of Mg and its alloys, which is attributed to the Mg's hexagonal close packed (hcp) crystal structure, is a major impediment and hence a number of studies were devoted to finding ways to alleviate it. Published literature shows that it can be achieved through the control of texture [3], microstructural refinement via thermo-mechanical processing [4–7], and through alloying [8]. Amongst the alloying options, Li appears to be a natural choice, especially since there is no weight penalty to Mg upon alloying with it. Consequently, a number of studies explored alloying Mg with Li. It is widely reported that the addition of Li promotes cross-slip and non-basal slip in Mg [9–11], making it more workable. Li addition decreases critical resolved shear stress (CRSS) for non-basal slip [12,13]. The decrease in CRSS (basal slip) due to Li addition (up to 1.8 wt%) is higher than that of Al and Zn, however, higher additions of Li increase athermal component of shear stress, τ_G, significantly. For example, an increase in the Li content from 2.0 to 3.0 wt% increases τ_G from ~2.5 to ~25 MPa [13]. First principles calculations [14] show that Li increases the stacking fault energy (SFE) of basal plane in Mg from 33 to 46 mJ/m^2, thus making cross-slip easier, whereas Al decreases it from 33 to 23 mJ/m^2. It is expected that the addition of Al stabilizes the extended dislocation configuration while Li tends to constrain the separation such that other dislocation processes (e.g. cross-slip) might become favourable. On the basis of the studies conducted to examine the effect of solutes (Al and Zn) on CRSS, Dorn [15] and Akhtar et al. [16] concluded that at lower T, the rate controlling process for deformation of Mg is Peierls' stress and cross-slip of screw dislocations at high T. In case of Mg-Li alloys, Dorn [15] concluded that rate controlling

---

[*] Corresponding author at: Department of Materials, Indian Institute of Science, Bangalore 560012, India.
E-mail address: ramu@materials.iisc.ernet.in (U. Ramamurty).

http://dx.doi.org/10.1016/j.msea.2016.03.087
0921-5093/

mechanism to be Peierls stress at all the T as cross-slip is easy due to increase in SFE for prismatic planes.

The Mg–Li system is of great interest because it not only offers the potential to substantially lower the density (Li – 0.58 g/cc vs. Mg – 1.74 g/cc) of the Mg upon alloying, but also improves the room-temperature (RT) ductility of Mg. The equilibrium phase diagram of the Mg-Li binary system is shown in Fig. S1 of the Supplementary information (SI) material. From it, we note that above ~5 wt% Li, a duplex alloy containing body centred cubic (bcc) β-phase is obtained and above ~11 wt% Li the alloy is entirely β [17]. The β-phase is soft and ductile, hence, the high Li alloys are ductile. However, they suffer from low temperature instability. Even the solid solution α-phase alloys show improved ductility and, notably, the ductile to brittle transition temperature in them is suppressed to below the liquid nitrogen temperature [18]. This phenomenon was linked to an increased activity of $[1\bar{2}10]$ $\{10\bar{1}0\}$ or prismatic $<a>$ slip system [18]. Li addition decreases the c/a ratio of Mg which is another factor contributing to the observed decrease in the CRSS for the non-basal slip [19].

Although a number of studies were conducted on the effect of Li addition on Mg's deformation response, as summarized in the preceding paragraph, the role of Li on improving the workability of Mg was not examined hitherto. As mentioned already, one of the main bottlenecks for the widespread use of Mg alloys in the wrought form is their relatively poor workability. Keeping this in view, we examine the effect of Li addition on the deformation behaviour of AZ31, a dilute and widely used Mg alloy, over the temperature range 150–400 °C. We also vary the Li content in the alloy between 1 and 5 wt% so as to examine the optimum Li content that results in best hot workability. The maximum Li added is kept at 5 wt% such that the focus is only on hcp α-phase, which is done keeping in view that the mechanical stability of the bcc phase is reportedly poor [20].

2. Materials and experiments

It is well known that Li is a highly reactive element and has low vapour pressure, therefore its handling requires special care. Li gets oxidized instantaneously when it comes in contact with the air. Further, the oxide products are powdery and do not protect the metal beneath. Hence, Li is stored under kerosene or under positive pressure of argon. In the present work, Li pieces of suitable size (or weight) are cut under the cover of kerosene. These cut pieces are immediately wrapped in the pre-weighed Al foils and finally stored in kerosene. During melting these pieces are dried in air to evaporate away kerosene and plunged into the melt along with the Al foil. Because of its lower density, molten Li on plunging into the melt can float on the surface of molten Mg and catch fire. Accordingly, utmost care is necessary during the addition of Li into Mg melt. Immediately on addition of Li, melt is stirred well to dissolve molten Li, also the flow rate of the protective gas (Ar+HFC 134a (Tetra fluoroethane)) is increased during stirring.

A special set-up was fabricated for melting and casting of Li containing compositions with provision for melting under protective atmosphere, a schematic of which is displayed in Fig. S2. Pouring was carried out in air. To protect the molten stream from oxidation and burning, a stream of protective gas is continuously purged over. Four compositions were selected to study the effect of Li on AZ31 Mg-alloy: 0, 1, 3 and 5 wt% Li. Henceforth, these are referred to as 0Li, 1Li, 3Li and 5Li, respectively. An electrical resistance heating furnace was used for preparation of the alloys. The following procedure was utilized. Pure Mg (98.5 wt% purity), pure Al (99 wt% purity), Al-10 wt% Mn master alloy were charged initially in the preheated melting crucible. All the charge materials are also preheated to drive away moisture. Argon gas was continuously passed into the crucible to protect the charge from oxidation and burning. On melting of the charge material, when T reaches ~ 700 °C, Zn (99% purity) was added to the melt, followed by a gentle stirring to disperse the Zn in the melt. Mg-30% Ca master alloy was also added to prevent the burning of liquid metal after Zn addition. Ca not only prevents the burning of liquid metal but also acts as a potent grain refiner in Mg-Li alloys [21,22]. Li (99.7% purity) was then added under increased flow rate of protective gas mixture. Molten alloys were poured into a metallic die of size 100×100 mm^2 cross-section and 200 mm depth under protective atmosphere of argon gas. As a result, no burning was observed during the melting and casting cycles. Ingots of the alloys were taken out of the die and homogenized at 400 °C for 24 h followed by air cooling. The homogenization cycle was arrived at on the basis of the isothermal section of the Mg-Al-Li phase diagram at 400 °C (Fig. S3) [23]. The ternary phase diagram reveals that at 400 °C all the alloying elements are in solid solution forming single phase (α-Mg). Protective atmosphere of argon was also maintained during the homogenization of the cast ingots.

Cylindrical compression test samples (8 mm in diameter and 12 mm in height) were machined from the homogenized ingots. Faces of these samples were provided with ring grooves of depth 0.5 mm for lubrication with graphite. Hot compression tests were carried out in a computer-controlled servo-hydraulic testing machine (DARTEC, West Midland, UK). The machine is equipped with an exponentially decaying cross head speed, enabling constant $\dot{\varepsilon}$ in the range of 10^{-3}–10^{+2} s^{-1} to be imposed on the specimens. Tests were carried out with T varying between 150 and 400 °C with 50° intervals and $\dot{\varepsilon}$ varying from 10^{-3} to 10^{+2} s^{-1}. This combination of T and $\dot{\varepsilon}$ encompasses the entire warm and hot working regime possible in Mg alloys. Specimens were heated in a split type resistance heating furnace with the T being monitored by a thermocouple attached to the sample. The accuracy of T control is within ±2 °C. Samples were soaked for additional 10 min prior to test at the prescribed T. Graphite powder was used for lubrication on sample faces to minimize barrelling during compression testing. Samples are compressed up to a total true strain, ε, of 0.6. Deformed samples were water-quenched immediately after completion of the tests. The load-displacement curves obtained at various T-$\dot{\varepsilon}$ combinations are converted into true stress (σ) vs. true strain (ε) curves after subtracting the elastic strain. Note that we have not corrected flow stress for adiabatic temperature rise. For metallographic examination, deformed samples are sectioned longitudinally in the direction parallel to the compression axis and are polished and etched with acetic-picral [5 ml acetic acid+6 g picric acid+10 ml H_2O+100 ml ethanol (95%)].

3. Results

Fig. 1(a)–(d) shows the representative microstructures of the Li containing alloys in the as-homogenized condition. They reveal the absence of the non-equilibrium phases that form during solidification. Measured grain sizes of alloys, listed in Table 1, indicate that the addition of Li to AZ31 Mg-alloy refines the microstructure. However, the variability in the grain size increases markedly upon the addition of Li. A few precipitates of $Mg_{17}Al_{12}$ and Al-Mn are seen in the micrographs of these alloys. However, we admit that the presence of Li containing precipitates cannot be ruled out on the basis of optical microscopy.

The chemical composition of various alloy ingots examined in the present work are summarized in Table S1. It reveals excellent yield with respect to Li content as the final values were close to the targeted compositions. A loss of ~10% was observed in the Li for alloys containing 1 and 3 wt% Li. Alloy with 5 wt% Li, however exhibited 20% loss due to oxidation. Yield for Al, Zn and Mn